

See discussions, stats, and author profiles for this publication at: <https://www.researchgate.net/publication/224492962>

Formation mechanism of alumina nanotubes and nanowires from highly ordered porous anodic alumina template

Article in *Journal of Applied Physics* · March 2005

DOI: 10.1063/1.1846137 · Source: IEEE Xplore

CITATIONS

17

READS

37

8 authors, including:



Pinyu Chen

University of Oregon

155 PUBLICATIONS 1,818 CITATIONS

[SEE PROFILE](#)



Hung TF

City University of Hong Kong

67 PUBLICATIONS 1,567 CITATIONS

[SEE PROFILE](#)



Yuanyuan Yang

Stony Brook University

283 PUBLICATIONS 6,169 CITATIONS

[SEE PROFILE](#)

Some of the authors of this publication are also working on these related projects:



Perovskite NCs Coating [View project](#)

Formation mechanism of alumina nanotubes and nanowires from highly ordered porous anodic alumina template

Y. F. Mei,^{a)} G. G. Siu, Ricky K. Y. Fu, P. Chen, X. L. Wu, T. F. Hung, and Paul K. Chu
Department of Physics and Materials Science, City University of Hong Kong, Kowloon, Hong Kong, China

Y. Yang^{b)}
State Key Laboratory of Coordination Chemistry, Department of Chemistry, Nanjing University, Nanjing, Jiangsu 210093, China

(Received 4 June 2004; accepted 18 November 2004; published online 6 January 2005)

Alumina nanotube (ANT) and nanowire (ANW) arrays were produced from highly ordered porous anodic alumina (PAA) by etching in phosphoric acid and subsequent thermal treatment. The domain structures that have small sizes provide more boundaries and break the hexagonal symmetry of the PAA template, thereby inducing star-like splitting modes. Using very thin PAA films, ANTs and their arrays are fabricated, whereas ANWs and their arrays are produced when using thick films. This is due to the thin wall between nanopores. Our results provide some mechanistic and fundamental information pertaining to the fabrication of nanostructures via a PAA template. © 2005 American Institute of Physics. [DOI: 10.1063/1.1846137]

I. INTRODUCTION

Recently, alumina nanostructures^{1–5} and their arrays^{6,7} have attracted much attention because of their potential applications in electrochemical processes and catalyses.¹ Alumina nanotubes (ANTs) as special nanostructures have been synthesized by several methods, including the hydrothermal reaction method,¹ coating of carbon nanotubes with aluminum isopropoxide,² anodization of Si-based alumina films in dilute sulfuric acid,^{4,7} and etching of a porous anodic alumina (PAA) template.⁵ In particular, anodization^{4,7} is more practical on account of the controllability, efficiency, and low cost. However, the electrochemical synthesis of ANTs and their arrays has only been based on anodization of Si-based aluminum films of high purity.⁷ If, on the other hand, ANTs can be produced from bulk aluminum, which is, incidentally, always used to fabricate highly ordered PAA templates,⁸ a myriad of novel nanostructures such as nanocables and nanofibers can be produced.

In the work described here, we produce highly ordered PAA templates by a well-controlled, two-step anodization process. After thermal treatment, the PAA template is observed to split in some local regions and ANTs are subsequently produced. Using the synthesis method, ANT and alumina nanowire (ANW) arrays can be produced on a thin PAA film on bulk aluminum.

II. EXPERIMENTS

High-purity Al sheets (99.99%) that had not been electropolished were first cleaned and anodized in sulfuric acid (15 wt %) using a constant dc voltage of 20 V at a temperature of $\sim 0^\circ\text{C}$ for 8–10 h to form the surface PAA film. After chemically removing the surface film in a mixture of phos-

phoric acid (6 wt %) and chromic acid (1.8 wt %), anodization was performed again under the same conditions for several hours to produce PAA with 25, 50, and 90 nm nanopores without electropolishing. The surface of the PAA was characterized by a JEOL JSM-6300 scanning electron microscope (SEM). Figure 1(a) depicts a typical SEM image of the highly ordered PAA template after immersion in sulfuric acid. It can be seen that the PAA has a perfect hexagonal nanopore arrangement in one domain with a pore diameter of about 25 nm and interpore distance of about 50 nm. The domains exhibit polycrystalline structure in which the structures show random orientation and shape. In order to produce alumina nanostructures, thermal treatment (100°C , 10–20 min, in air) was adopted for PAA films with various thickness after the enlargement of the nanopores by immersing the samples in 5 wt % phosphoric acid for 30 min.

III. RESULTS AND DISCUSSION

This domain morphology has been observed in previous works.^{9–11} Since the crystalline grains of aluminum are much larger than the domain size, there is no correlation between each other.¹² In our work, the domain size is found to be about 200–1000 nm in all the samples prepared under the same conditions but with different anodization time, but that reported in Li's work was about 1–5 μm .^{9,10} Nielsch *et al.*¹¹ have suggested that there is an optimal anodization time to obtain the largest domain size. In our experiments, different anodization times varying from 30 min to 20 h were attempted, but no obvious changes in the domain size could be observed.

A mechanism to explain the self-organization was suggested by Jessensky¹³ as follows. The resulting mechanical stress at the metal/oxide interface is proposed to give rise to repulsive forces between the neighboring pores, thereby promoting the formation of ordered hexagonal pore arrays. Based on our results and previous works by others and

^{a)}Electronic mail: meiyongfeng@nju.org.cn, yf.mei@plink.cityu.edu.hk

^{b)}Now at Graduate School of Material Science, University of Hyogo, Japan.

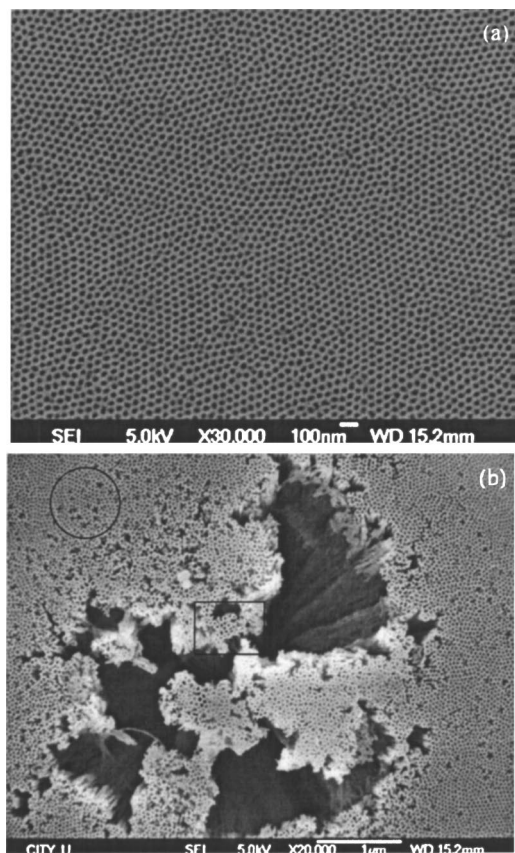


FIG. 1. SEM images of the PAA template: (a) with highly ordered arrangement formed in sulfuric acid solution (15 wt %) under dc constant voltage (20 V) at a temperature of $\sim 0^\circ\text{C}$ and (b) with some cracks after immersion in 5 wt % phosphoric acid for 30 min and thermal treatment (100°C , 10–20 min, in air).

ourselves,^{9–14} it is suggested that the maximum domain size is different in PAA films obtained under different conditions due to the intrinsic feature of the PAA film. It may be affected by the mobility of ions, microstructure and surface structure of aluminum, and repulsive forces between the neighboring pores; more work must be performed to fully understand the mechanism.

After the enlargement of the nanopores by immersing the samples in 5 wt % phosphoric acid for 30 min and thermal treatment (100°C , 10–20 min, in air), several distinctive regions as shown in Fig. 1(b) can be observed. Some tube-shaped features can be observed [labeled with a rectangle of Fig. 1(b)]. However, the formation of ANTs appears to be different from that observed in our previous work. In our previous work,^{7,14} the cell structures play an important role in the formation of ANTs on Si-based PAA films and one individual ANT corresponds to one cell. The cleavage of the D-D route is responsible for the formation of the ANTs and their array.⁷ The intrinsic factors are the microstructure of the Si-based PAA film and polycrystalline structure with sizes of 100–1000 nm in the Al film, while the extrinsic factor is the pulsed dc voltage.¹⁴ Previously,⁵ due to the nonuniform pore size and the disordered pore distribution in the PAA film, ANTs and ANWs were produced by etching in dilute NaOH solution. However, the PAA used in the present experiments is highly ordered. The formation of ANTs appears to be due

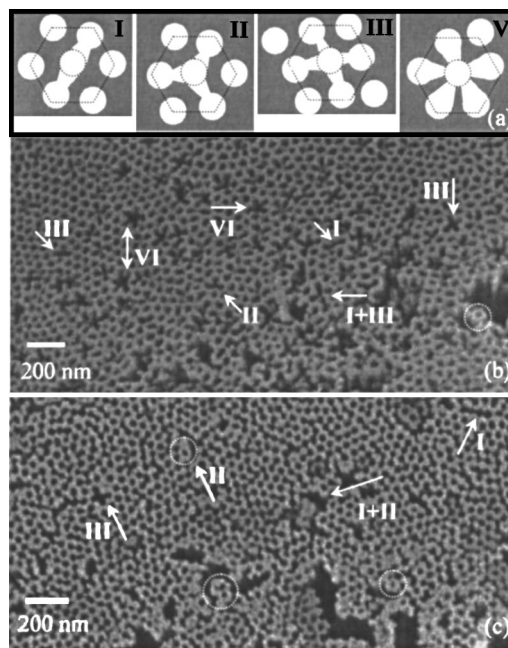


FIG. 2. (a) Schematic diagrams of the splitting modes (modes I, II, III, and VI). (b) and (c) SEM images of PAA templates with cracks.

to the splitting of the nanopores itself as an individual ANT is formed by splitting the nanopores around it. In addition, there are some star-like cracks in the vicinity of the large splits [shown in a big circle in Fig. 1(b)] such as the five-point stars that are important to the formation of ANTs from Al-bulk-based PAA films; these should be investigated further.

As shown in Fig. 2(a), four types of splitting modes, individually named as modes I, II, III, and VI, can be observed. These modes are based on the variation of the inter-pore distance. The splitting of the central nanopore to six neighboring pores depends on the thickness of the wall and stress between them. In this work, only the thickness of the wall is considered because the stress¹¹ on a nanoscale is hard to identify. The thinner the wall between two neighboring nanopores, the easier is the split. After the heat treatment, splitting results due to the volume expansion and stress release.¹³ It should be noted that the splitting process is not unique. Splitting can occur via route 2-0-4, 3-0-4, 1-0-4, or others [0, 1, 2, 3, 4, 5, and 6 correspond to each nanopore as shown in mode I of Fig. 2(a)] if the conditions are met. As illustrated in Figs. 2(b) and 2(c), single modes and their combinations can be easily checked. Some individual ANTs [refer to the circles in Figs. 2(b) and 2(c)] have been formed in some split regions as a result of the combination mode.

The reason for these four splitting modes may be the break of the hexagonal symmetry in PAA. As reported earlier,⁷ the polycrystalline structure is a key factor during the formation of Si-based ANT arrays because the polycrystal yields domain structures with very small size. A small domain structure breaks the hexagonal symmetry of the PAA film. Thus, not only ANTs can be formed, but their array with uniform size can also be produced using a pulsed voltage.¹⁴ So far, the grain size of bulk aluminum¹² is much larger than the domain size of the PAA template. The domain

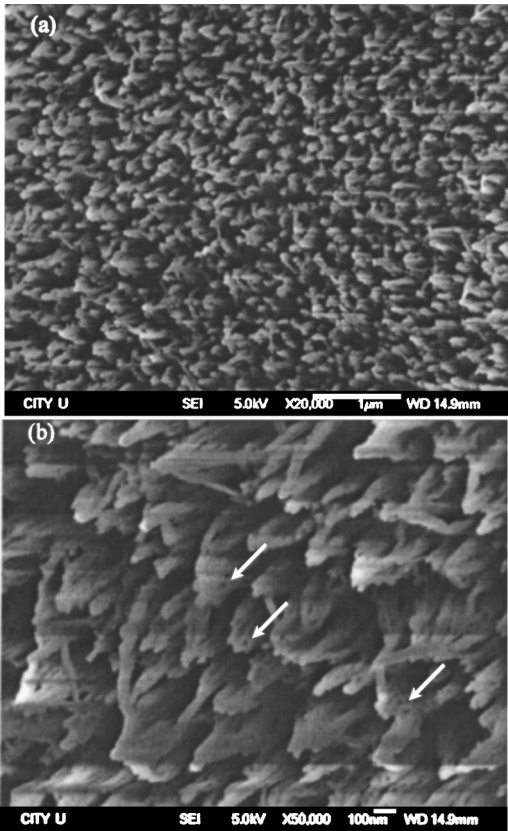


FIG. 3. (a) SEM image of ANT array on bulk-Al-based PAA template with a thin film. (b) Magnified SEM image.

size reported here is similar to that reported in our previous work.⁷ It was induced by the polycrystalline structure of the thin aluminum film and was smaller than those reported by other groups.^{9–11} Different domain structures in one of the PAA films exhibit different shapes and orientations. The domain boundary seriously affects the arrangement of the nanopores. A smaller domain size implies more domain boundary, and that results in higher disruption of the hexagonal symmetry in bulk-Al-based PAA films. Once the symmetry is broken, the splitting of the nanopore can take place since some extrinsic factors such as volume expansion, thinning of the wall between the nanopores, and others become important.

By adopting the mechanism involving the different splitting modes, a large quantity of ANTs (several square millimeters) and their array can be fabricated by a modified method. The procedure is similar to the fabrication of PAA template, but the anodization time in the second step is short (about 5 min). The calculated anodization rate is about 200 nm/min under our conditions, so that the final thickness of the PAA template is about 1000 nm. After the highly ordered PAA template was immersed in 5 wt % phosphoric acid for several minutes followed by thermal treatment at 100 °C for 10–20 min in air, ANTs arrays were obtained as demonstrated in Fig. 3(a). The ANT array is observed to be quite uniform and numerous. The diameter of the ANT is about 50–60 nm and the length is shorter than 1000 nm because of the etching effect by phosphoric acid. The enlarged image in Fig. 3(b) shows an individual ANT (see the white arrow).

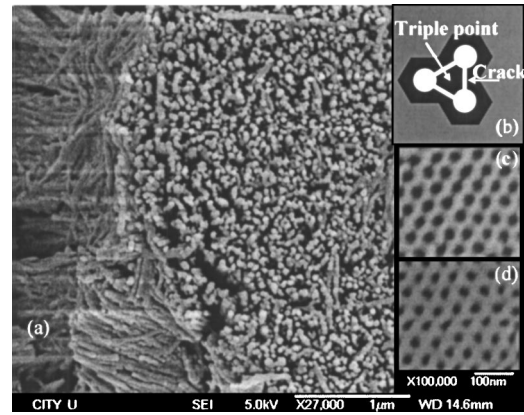


FIG. 4. (a) SEM image of alumina nanowire array. (b) Schematic diagrams showing the formation of ANW from triple point of the PAA template. (c) SEM images of PAA templates with highly ordered arrangement near the surface. (d) SEM images of PAA templates with highly ordered arrangement on the bottom showing different nanopore sizes.

For the ratio of ANTs, we consider it as 10% of whole alumina nanostructures (including ANTs and ANWs) from our SEM measurement and Fig. 3. A uniform ANW and ANT array could not be fabricated with thick PAA film due to its discrete crack depths. However, it can be accomplished with thin film because the cracks were prevented by the pure Al substrate because of short path to crack.

The thickness of the PAA film can influence the result of either the ANT or ANW arrays. When the thickness of the PAA film is much thicker than 1000 nm, very few ANTs can be formed while ANWs and their array are always obtained. A typical image is shown in Fig. 4. The diameter of the ANW is about 30–40 nm, which corresponds to the thickness of the wall between the nanopores. Here, the formation of one individual ANW can be attributed to the splitting of walls surrounding three nanopores,⁶ as shown in Fig. 4(b). For a long anodization time, the nanopore on the surface of PAA film is larger than that at the interface between the PAA film and Al substrate [Figs. 4(c) and 4(d)]. It implies that the wall between the nanopores is thinner in the near-surface region compared to that underneath. Figure 4(c) displays the surface image of the PAA film and Fig. 4(d) shows the bottom image of the PAA film. It is obvious that the nanopores in the near-surface region are larger than those underneath. The thin wall results in splitting between nanopores and generally, splitting is more likely to be initiated by the nanopores at the surface. If most of the walls are split, more nanowires can be formed.

IV. CONCLUSIONS

To recapitulate, ANTs, ANWs, and their arrays were obtained on bulk aluminum by an efficient and economical anodization method. Several splitting modes that break the hexagonal symmetry play an important role during the formation of alumina nanostructures. The significance for our work is that some nanostructures can be formed on the PAA template itself without the need to embed materials.

ACKNOWLEDGMENTS

The authors thank Dr Amy X. Y. Lu for her help. This work was supported by Hong Kong Research Grants Council (RGC), Competitive Earmarked Research Grant (CERG) #CityU 1052/02E, as well as Hong Kong RGC - Chinese NSFC Research Grant #N_CityU 101/03.

¹H. C. Lee, H. J. Kim, S. H. Chung, K. H. Lee, H. C. Lee, and J. S. Lee, *J. Am. Chem. Soc.* **125**, 2882 (2003).

²Y. J. Zhang, J. Liu, R. R. He, Q. Zhang, X. Zhang, and J. Zhu, *Chem. Phys. Lett.* **360**, 579 (2002).

³J. S. Lee, B. Min, K. Cho, S. Kim J. Park, Y. T. Lee, N. S. Kim, M. S. Lee, S. O. Park, and J. T. Moon, *J. Cryst. Growth* **254**, 443 (2003).

⁴L. Pu, X. M. Bao, J. P. Zou, and D. Feng, *Angew. Chem., Int. Ed.* **113**, 1538 (2001).

⁵Z. L. Xiao, C. Y. Han, U. Welp, H. H. Wang, W. K. Kwok, G. A. Willing,

J. M. Hiller, R. E. Cook, D. J. Miller, and G. W. Crabtree, *Nano Lett.* **11**, 1293 (2002).

⁶Z. H. Yuan, H. Huang, and S. S. Fan, *Adv. Mater. (Weinheim, Ger.)* **14**, 303 (2002).

⁷Y. F. Mei, X. L. Wu, X. F. Shao, G. G. Siu, and X. M. Bao, *Europhys. Lett.* **62**, 595 (2003).

⁸H. Masuda and K. Fukuda, *Science* **268**, 1466 (1995).

⁹A. P. Li, F. Müller, A. Birner, K. Nielsch, and U. Gösele, *J. Appl. Phys.* **84**, 6023 (1998).

¹⁰A. P. Li, F. Müller, A. Birner, K. Nielsch, and U. Gösele, *J. Vac. Sci. Technol. A* **17**, 1428 (1999).

¹¹K. Nielsch, J. S. Choi, K. Schwirn, R. B. Wehrspohn, and U. Gösele, *Nano Lett.* **7**, 677 (2002).

¹²O. Jessensky, F. Müller, and U. Gösele, *J. Electrochem. Soc.* **145**, 3735 (1998).

¹³O. Jessensky, F. Müller, and U. Gösele, *Appl. Phys. Lett.* **72**, 1173 (1998).

¹⁴Y. F. Mei, X. L. Wu, X. F. Shao, G. S. Huang, and G. G. Siu, *Phys. Lett. A* **309**, 109 (2003).